MIT Open Access Articles

Temperature#dependent vapor–liquid equilibria and solvation free energy estimation from minimal data

Temperature dependent vapor-liquid equilibria and solvation free energy estimation from minimal data

Yunsie Chung[1]* | Ryan Gillis[1]* | William H. Green[1]

[1]Department of Chemical Engineering, Massachusetts Institute of Technology, Cambridge, MA, 02139, U.S.A

Correspondence

William H. Green, Department of Chemical Engineering, Massachusetts Institute of Technology, Cambridge, MA, 02139, U.S.A
Email: whgreen@mit.edu

We present a new strategy to estimate the temperature dependent vapor-liquid equilibria and solvation free energies of dilute neutral molecules based on only their estimated solvation energy and enthalpy at 298 K. These two pieces of information coupled with matching conditions between the functional forms developed by Japas and Levelt Sengers for near critical conditions and by Harvey for low and moderate temperature conditions allow the fitting of a piecewise function that predicts the temperature dependent solvation energy for dilute solutes up to the critical temperature of the solvent. If the Abraham and Mintz parameters for the solvent and solute are available or can be estimated from

group contributions, this method requires no experimental data and can still provide accurate estimates with an error of about 1.6 kJ/mol. This strategy, which requires minimal computational resources, is shown to compare well with other methods of temperature dependent solvation free energy prediction.

INTRODUCTION

Predicting solvation's effects on the thermochemistry of dilute solutes is of great importance to numerous industrial and environmental efforts. Partitioning coefficients between fluid phases are needed for the design of synthesis and separation processes, the prediction of biomolecular properties, and the management of pollutant levels affecting human health.[1,2,3] Rapid, accurate solvation energy predictions are also key to the creation of detailed chemical mechanisms that enable us to understand complex reacting systems. Most ab initio thermochemistry calculations and experimental measurements rely on a gas phase environment, requiring solvation thermochemistry corrections for any system in a condensed phase.

Many methods for predicting solvent effects on the thermochemistry of solutes have been developed. These range in complexity from simple linear models, like those created by Abraham[4] and Mintz,[5] to methods based on quantum calculations, such as those developed by Cramer and Truhlar[1] or Klamt.[6] Simple linear models are trivial to calculate once fit to experiments but are necessarily limited by the information that they predict, that is, solvation properties at a single pressure and temperature. Most solvation data are obtained at 1 bar and 298 K, and high temperature measurements are scarce. While one can extrapolate to other conditions using these values, the predictions become

drastically less accurate as the temperature diverges from where the model was fit to experiments. The UNIQUAC

activity coefficient models are widely used to predict phase equilibria across a range of temperatures. However, they

typically rely on fitted empirical parameters specific to the solute and solvent pairs.[7] The UNIFAC method modifies

this approach by using the functional groups in the solute and solvent to predict the model parameters, reducing the

need for fitted empirical parameters for every unique pair. It is however, limited in the types of molecules for which the

predictions can be made.[8, 9, 10] In either method, one relies on temperature dependent data either directly worked into

the binary interaction parameters or upon which the temperature dependent functional group predicted parameters are

based.[10] Semi-empirical correlations developed by Plyasunov et al.[11, 12] exist for predicting solvation properties across

wide ranges of temperature and pressure, but their studies were limited to aqueous solution and required empirically fit

parameters.

In contrast, ab initio methods can predict solvation properties without any experimental data but can require

extensive computational resources. Further, the temperature ranges in which they are reliable are often limited by the

experimental conditions of the training set used to parameterize the solvation models. For example, the SMD model[13]

based on the interaction between the quantum mechanical electron density of solutes and continuum solvents is known

for its ability to predict solvation free energies for neutral or charged solutes in solvents at 298 K with great accuracy.

However, the model is trained with experimental data at 298 K and therefore not suitable for higher temperature

calculations. The COSMO-RS[6] is another widely used continuum solvation model that combines both quantum and

statistical mechanics to predict solvation thermochemical properties for any solutes in a wide variety of solvents. The

COSMO-RS model accounts for the temperature dependence of solvation properties both implicitly through statistical

thermodynamics and explicitly through temperature dependent parameters for liquid-gas transfer, van der Waals

forces, and hydrogen bonding and thus can calculate these properties as a function of temperature.[14] However since

the assumptions made in the explicit temperature dependence correlations are relatively simple, the predictions are

most accurate near room temperature and the error is expected to increase as the temperature significantly deviates

from 298 K.

Whatever the adopted strategy, trade-offs between accuracy, computational expense, and range of compatible

molecules must be navigated. In this work we demonstrate a method for predicting the temperature dependent

solubilities, and hence solvation free energies, of neutral solutes in dilute solvent systems. We believe that such a method is particularly useful for applications where the speed of property calculation is more important than extreme accuracy. The automatic creation of detailed chemical mechanisms is one such application with these needs. However, the method can be of use to anyone that seeks to predict solute partitioning or solvation thermochemistry for systems at elevated temperatures if corresponding high temperature measurements are not available.

The method involves fitting a piecewise function to predicted Gibbs free energies and enthalpies of solvation at 298 K. It provides an estimate of the vapor-liquid equilibrium ratio and solvation energy up to the critical temperature of the solvent. Infinite dilution conditions are assumed. Further, the pressure dependence of solvation properties is neglected in this technique, limiting the method to moderate and low pressure systems. Significant error is anticipated for high pressure systems or systems with large solute molecules for which the pressure dependence of solvation can be significant.[15]

RELEVANT SOLVATION THERMODYNAMIC RELATIONSHIPS

| Definitions and Functional Forms of Temperature Dependence

Gas solubilities in solution are commonly expressed in terms of a Henry's constant, k_{H}. The Henry's constant of a solute (component 2) in a solvent (component 1) at temperature T and pressure P is defined by[16]

$$k_{\mathrm{H}}(T, P) = \lim_{x_2 \to 0} \frac{f_2(T, P, y_2)}{x_2} \tag{1}$$

where f_2, y_2, and x_2 are the fugacity, vapor phase mole fraction, and liquid phase mole fraction of the solute respectively. If the vapor phase is dilute enough, non-ideality becomes negligible and the fugacity of the solute is equal to the partial

pressure of the solute and the Henry's constant becomes

$$k_H(T, P) \approx \lim_{x_2 \to 0} \frac{P y_2}{x_2} \tag{2}$$

Another related term is the K-factor, $K_{2,1}$, which is also known as the vapor-liquid equilibrium ratio. It is defined as the ratio of the equilibrium mole fractions of the solute in the gas and liquid phases

$$K_{2,1}(T, P) = \frac{y_2}{x_2} \tag{3}$$

At infinite dilution of the solute, K-factor becomes

$$K_{2,1}^\infty(T, P) = \lim_{x_2 \to 0} \frac{y_2}{x_2} \approx \frac{k_H}{P} \tag{4}$$

In 1989, Japas and Levelt Sengers derived an asymptotic relationship for infinite dilution K-factor ($K_{2,1}^\infty$) near the solvent's critical temperature, T_c, based on first principles:[16]

$$T^* \ln(K_{2,1}^\infty(T)) = D \left(\frac{\rho_1^l(T)}{\rho_{crit,1}} - 1 \right) \tag{5}$$

where ρ_1^l, $\rho_{crit,1}$, and D each represent the molar density of the pure liquid-phase solvent at the solvent's saturation pressure, the critical molar density of the pure solvent, and an empirical parameter. T^* is the reduced temperature, $\frac{T}{T_c}$. The K-factor in this relationship was calculated along the solvent's saturation curve and thus is only a function of temperature.[17] A number of studies have revealed that this asymptotic linear behavior is ubiquitous in dilute solution systems and can be extended from the critical temperature to temperatures as low as 400 K for some systems.[18,19]

Harvey later proposed a semi-empirical 3-parameter correlation for Henry's constants[18]

$$\ln \left(\frac{k_H(T)}{P_1^{sat}(T)} \right) = \frac{A}{T^*} + B \frac{(1 - T^*)^{0.355}}{T^*} + C \frac{\exp(1 - T^*)}{(T^*)^{0.41}} \tag{6}$$

where P_1^{sat} is the solvent's saturation pressure, and A, B, and C are empirical parameters specific to the solvent-solute pair. Henry's constant in this equation is also calculated at the solvent's saturation curve and therefore only a function of temperature. Harvey's equation provides more accurate estimations for a wider temperature range from around 298 K to close to the critical point.[18] The only caution is that it should not be used for temperatures within 1 % of the solvent's critical point. However, the method requires experimental data across the temperature range to fit 3 parameters for each solute-solvent pair, and these data are usually unavailable. Moreover, the accuracy of the correlation can vary depending on the abundance and quality of the typically scarce data.

If ideal gas behavior of the solute is assumed at dilute limit, equation (6) becomes

$$\ln\left(\frac{K_{2,1}^{\infty}(T)P}{P_1^{sat}(T)}\right) = \frac{A}{T^*} + B\frac{(1 - T^*)^{0.355}}{T^*} + C\frac{\exp(1 - T^*)}{(T^*)^{0.41}} \tag{7}$$

which holds for any gas mixture and total pressure P as long as all the dissolved gases are in the dilute limit. If the K-factor is evaluated along the solvent's saturation curve, the pressure terms, P and P_1^{sat}, cancel out.

| Predicting Solvation Properties at 298 K with Linear Models

Other recent studies on solvation thermochemistry have focused on developing models to predict gas-liquid equilibria at room temperature. The Abraham linear solvation energy relationship (LSER) method uses solute and solvent parameters, represented by the uppercase and lowercase letters respectively, to estimate the partition coefficient[4]

$$\log_{10} K(298\text{ K}) = c + eE + sS + aA + bB + lL \tag{8}$$

where the partition coefficient is the ratio of equilibrium concentrations of the solute in liquid and gas phases.

$$K = \frac{c_{2,\text{liquid}}}{c_{2,\text{gas}}} \tag{9}$$

Numerous solute and solvent descriptors have been tabulated based on experimental data.[4, 20, 21, 22] The descriptors of missing solute species can be obtained from the group additivity method devised by Platts et al.[23] or other resources such as UFZ-LSER database.[24]

The free energy of solvation for a dilute solute can be calculated from its equilibrium concentration in the gas and liquid phases. In this work, we define the solvation free energy as a change in the Gibbs free energy of a solute associated with the transfer of a solute molecule from a dilute gas phase into a dilute liquid phase at constant T and P. Both gas and liquid phases in this solvation process are binary mixtures of a solvent and a solute. By using the standard-state of the gas and solution at equal and dilute solute concentrations similar to the Ben-Naim standard state,[25] one can directly calculate the free energy of solvation with equation (10).

$$\Delta G^*_{solv} = -RT \ln(K) \tag{10}$$

At dilute limit, solvation free energy can be related to the K-factor using the pure solvent's properties:

$$\Delta G^*_{solv} = RT \ln\left(\frac{K^\infty_{2,1}\rho^g_1}{\rho^l_1}\right) \tag{11}$$

where ρ^g_1 is the molar density of the pure gas-phase solvent.

Another linear solvation energy relationship (LSER) method has been developed by Mintz et al.[5] and uses the solvent and solute descriptors to estimate the enthalpy of solvation, ΔH^*_{solv}, at 298 K.

$$\Delta H^*_{\text{solv}}(298 \text{ K}) = c' + e'E + s'S + a'A + b'B + l'L \tag{12}$$

$$\Delta S^*_{\text{solv}}(298 \text{ K}) = \frac{\Delta H^*_{\text{solv}}(298 \text{ K}) - \Delta G^*_{\text{solv}}(298 \text{ K})}{298 \text{ K}} = -\frac{d\Delta G^*_{\text{solv}}}{dT}\bigg|_{T=298 \text{ K}} \tag{13}$$

These relationships provide widely applicable, quickly calculable values for solvation properties at 298 K.

| Temperature Extrapolation Methods

Solvation free energies at other temperatures are often extrapolated by assuming constant ΔH^*_{solv} and ΔS^*_{solv}.

$$\Delta G^*_{\text{solv}}(T) \approx \Delta H^*_{\text{solv}}(298 \text{ K}) - T\Delta S^*_{\text{solv}}(298 \text{ K}) \tag{14}$$

Coupled with methods to estimate the solvation enthalpy and entropy at 298 K, this represents a rapid, first-order approximation of the temperature dependence of solvation free energy.[26] However, since the actual solvation enthalpy and entropy vary with temperature, this approximation is only applicable for temperatures near 298 K.

A variation of the Van't Hoff Equation can also be used to extrapolate Henry's Law constants as suggested by Smith and others.[27,28]

$$\frac{k_H(T)}{k_H(298\ \text{K})} \approx \exp\left(\frac{\Delta H^*_{\text{solv}}(298\ \text{K})}{R}\left(\frac{1}{298\ \text{K}} - \frac{1}{T}\right)\right) \tag{15}$$

METHODS

| The Piecewise Function

Our proposed method centers around the fitting of a four parameter piecewise function that predicts K-factors as a function of temperature. The low temperature piece of the function has the three parameter form recommended by Harvey[18] while near the critical temperature the function is constructed according to the work of Japas and Levelt Sengers which has a single parameter.[16] The transition point between them was set empirically based on the validation set to 0.75 of the critical temperature of the solvent. The two functions are shown below in equation (16) and (17)

$$K^\infty_{2,1}(T \leqslant 0.75T_c) = \exp\left(\frac{A + B(1 - T^*)^{0.355} + C(T^*)^{0.59}\exp(1 - T^*)}{T^*}\right) \tag{16}$$

$$K_{2,1}^{\infty}(0.75T_c \leqslant T < T_c) = \exp\left(\frac{D}{T^*}\left(\frac{\rho_1^l(T)}{\rho_{\text{crit},1}} - 1\right)\right) \tag{17}$$

where ρ_1^l, the molar density of the pure liquid-phase solvent, is evaluated at the solvent's vapor pressure such that only the temperature dependence of the K-factor is considered.

We note that the piecewise structure of this prediction method is needed rather than simply extrapolating the linear part of Harvey's correlation at high temperature because the slope produced by such extrapolation deviates from the true asymptotic slope near the critical point as observed by Harvey et al.[29]

| Solving for the 4 Parameters

We obtain two equations by forcing the two pieces of the piecewise function to match in value and gradient at the transition temperature:

$$A + B(1 - T_{\text{tr}}^*)^{0.355} + C(T_{\text{tr}}^*)^{0.59}\exp(1 - T_{\text{tr}}^*) = D\left(\frac{\rho_1^l(T_{\text{tr}})}{\rho_{\text{crit},1}} - 1\right) \tag{18}$$

$$-\frac{0.355B}{T_c}(1 - T_{tr}^*)^{-0.645} + \frac{C\exp(1 - T_{tr}^*)}{T_c}\left(0.59(T_{tr}^*)^{-0.41} - (T_{tr}^*)^{0.59}\right) = \frac{D}{\rho_{crit,1}}\frac{d\rho_1^l}{dT}\bigg|_{T=T_{tr}} \tag{19}$$

where T_{tr}^* is the reduced temperature at the transition point ($T_{tr}^* = T_{tr}/T_c$), and the transition temperature, T_{tr}, is empirically chosen as $0.75T_c$ as previously mentioned.

Two additional equations can be obtained from either experimental data or linear solvation models. In this work, we used the Abraham[4] and Mintz et al.[5] LSERs to estimate the solvation free energy and enthalpy and calculate the K-factor and its temperature gradient at 298 K:

$$A + B(1 - T_{298\,K}^*)^{0.355} + C(T_{298\,K}^*)^{0.59}\exp(1 - T_{298\,K}^*) = T_{298\,K}^* \ln K_{2,1}^\infty(298\ K) \tag{20}$$

$$-\frac{0.355B}{T_c}(1 - T_{298\,K}^*)^{-0.645} + \frac{C\exp(1 - T_{298\,K}^*)}{T_c}\left(0.59(T_{298\,K}^*)^{-0.41} - (T_{298\,K}^*)^{0.59}\right) = \frac{d\left(T^*\ln K_{2,1}^\infty(T)\right)}{dT}\bigg|_{T=298\,K} \tag{21}$$

where $T_{298\,K}^*$ is the reduced temperature at 298 K ($T_{298\,K}^* = 298\ K/T_c$). The K-factor is calculated from the solvation free

energy by using equation (11), and the temperature gradient of the K-factor is calculated with finite differences from the enthalpy at 298 K. We used the Abraham and Mintz parameters obtained from Solvation Database in RMG[30] and M. H. Abraham through personal communication.[31] The Abraham parameters of the missing solutes are estimated by the Platts group additivity method implemented in RMG.[23]

By solving equations (18) - (21), we can find the four parameters (A, B, C, and D) of the piecewise function. This is an independent linear system with respect to the parameters and can be easily solved with a linear equation solver. All solvent's properties including the liquid-phase density and gas-phase density used in equation (11) are evaluated at the solvent's saturation pressure using CoolProp.[32] CoolProp is a free fluid modeling software based on Helmholtz energy equations of state. It provides accurate estimations of fluid properties over the wide ranges of temperature and pressure for a variety of fluids. The temperature gradient of the solvent's liquid-phase density in equation (19) is also computed from CoolProp using the finite difference method.

A sample code that uses our method is located at `https://github.com/ReactionMechanismGenerator/RMG-Py/tree/master/ipython/temperature_dependent_solvation_free_energy.ipynb`. A simple web-based calculator is also available on `https://rmg.mit.edu/database/solvation/search/`.

| Standardization of Data for Model Validation

Experimental data on vapor-liquid equilibrium (VLE) are usually given in x_2, y_2, T, and P, and therefore we have chosen to compare $K_{2,1}^\infty P$ up to the critical temperature for model validation. Note that this metric is equivalent to both $\frac{y_2}{x_2} P$ for experimental data where P is the experimental pressure and $K_{2,1}^\infty P_1^{\text{sat}}$ for our model along the saturation curve. Although these two notations use different pressures and the experimental K-factors are not at infinite dilution, we will refer to both these values as $K_{2,1}^\infty P$ for simplicity. Some experimental data were given only in Henry's constants (k_H), and it was often unclear how they were determined. We assumed that these values are most likely referring to $\frac{y_2}{x_2} P$ and directly compared them with our estimated $K_{2,1}^\infty P_1^{\text{sat}}$.

Since K-factors are less intuitive to compare and other existing methods predict solvation free energy, we have also chosen to compare solvation free energy. For our method, we calculated solvation energies from predicted K-

factors using equation (11). All relevant solvent properties were evaluated at the solvent's saturation pressure. The experimental VLE data (x_2, y_2, T, and P) were converted to solvation energies using the same equation, but the solvent's gas-phase density was evaluated at experimental pressure instead of at saturation pressure. We assumed negligible pressure effect on liquid density and used the solvent's saturated liquid density for experimental data conversion. The gas densities for a few experimental points could not be solved by the equations of state employed in CoolProp and these points were omitted from experimental solvation energy data. The omitted data are listed in the Supporting Information.

For the experimental data given as k_H, experimental P was not known. Therefore, we approximated solvation free energy using ideal gas law

$$\Delta G^*_{solv} \approx RT \ln \left(\frac{k_H}{RT\rho^l_1} \right) \tag{22}$$

where ρ^l_1 was evaluated at the solvent's saturation pressure. The ideal gas assumption would no longer be valid at high pressure and this may cause some error in high temperature regions where pressures are high.

We also examined the error introduced by using ideal gas assumptions when converting K-factors to solvation energies. In order to do so, solvation energies were calculated from the predicted K-factors using the ideal gas density as shown in equation (23) and compared with those calculated with non-ideal gas densities.

$$\Delta G^*_{solv} \approx RT \ln \left(\frac{K^\infty_{1,2} P^{sat}_1}{RT\rho^l_1} \right) \tag{23}$$

The methods and assumptions used to standardize the data to $K_{2,1}^\infty P$ and solvation free energies are summarized in the Supporting Information.

| COSMO-RS Calculations

The COSMO-RS calculations were performed using the software COSMOtherm version 1901.[33] Solvation free energies were computed from room temperature to near critical temperatures of solvents on both BP/TZVP and BP/TZVPD-FINE levels of theory. These calculations were done for the solute-solvent pairs whose pre-calculated quantum chemical results were available in the default COSMOtherm database. No quantum chemical COSMO calculations were performed in this work.

RESULTS

We calculated temperature dependent K-factors for 47 solute-solvent systems and compared them with the experimental data and predictions based on the Van't Hoff equation (equation 15). These experimental data were largely compiled in the Dortmund Databank integrated in SpringerMaterials[34] with detailed references to the original sources contained in the Supporting Information. The Henry's law constants (k_H) estimated from the Van't Hoff equation are approximated as $K_{1,2}^\infty P$ for comparison. We also compared predicted solvation free energies with the experimental data and predictions based on the Van't Hoff equation (equation 15 and equation 22), constant enthalpies and entropies (equation 14), and COSMO-RS TZVP and TZVPD-FINE methods (for 42 and 41 pairs with the BP/TZVP and BP/TZVPD-FINE levels respectively). The solvation free energies at 298 K obtained from Minnesota Solvation Database (MNSOL) version 2012[35] are also plotted along with other experimental data for the available solute-solvent pairs. The three extrapolating methods (the Van't Hoff, constant enthalpies and entropies, and our proposed method) were performed using $\Delta G_{solv}^*(298\,\text{K})$ and $\Delta H_{solv}^*(298\,\text{K})$ estimated from the Abraham and Mintz LSERs.

Figure 1 shows the results for 5 binary systems. The proposed method in Figure 1 uses non-ideal gas densities to compute solvation energies from the predicted K-factors (equation 11). The proposed strategy is superior to the other listed methods for most of the solvent/solute pairs, especially at elevated temperatures. The detailed results for all 47 solute-solvent pairs, including the plots for $\ln(K_{2,1}^{\infty})$ without the pressure term, can be found in the Supporting Information.

We calculated solvation energies using ideal gas densities as well and compared these with the more exact non-ideal calculations in Figure 2 for the same 5 binary systems. Note that for both non-ideal and ideal methods, solvation energies were calculated from the same K-factors, and the difference only arises from employing different gas densities of the solvent for the conversion between K-factor and solvation energy (using equation 11 for non-ideal densities and equation 23 for ideal gas densities).

We can quantitatively describe the accuracy of these methods with the deviation between the experimental data and method predictions. Table 1 below shows summary statistics for the comparison of methods. Figure 3 is a histogram of the root mean squared deviation between experiment and estimate using our proposed method with non-ideal gas densities and the COSMO-RS software at the BP/TZVPD-FINE level of theory.

Full information on the sources, types of experimental data used, maximum mole fractions, and maximum ratios of experimental pressure to saturated pressure is presented in the Supporting Information. The fitted parameters for all 47 solute-solvent pairs can be found in the Supporting Information as well. The original VLE data can be obtained from SpringerMaterials.[34]

DISCUSSION

Across a wide diversity of molecular properties in both solvents and solutes in our test sets, the general behavior of the K-factors and solvation energies is seen to be fairly consistent. This suggests that the phenomena governing solvation is constant regardless of the nature of the individual solutes or solvents.

In one sense the method we propose can be thought of as a very nuanced extrapolation from known solvation properties at 298 K to the critical point. However, this extrapolation is done with knowledge of the typical shape of

the K-factor/temperature curve and enforcing the correct asymptotic behavior near the critical point, rather than just naively assuming constant parameters. As a result, while other extrapolation methods start to deviate as temperature increases, our method approaches a correct limit.

Our strategy estimates the K-factors along the solvent's saturation curve. However, the validating experiments contain data whose pressure deviates significantly from the vapor pressure occasionally up to a factor of approximately 13 (see the Supporting Information). The continued accuracy of our $\ln(K_{1,2}^{\infty}P)$ and solvation energy predictions at these pressures seems to suggest that our model has predictive power across a range of pressures. Yet, this is a risky presumption to make. Most of the pressure deviation was observed at low temperatures where the pressure was also generally lower. Our method forces the predicted K-factor to match the value and gradient estimated from the Abraham and Mintz LSERs at 298 K, and these LSERs were developed based on the empirical data measured at atmospheric pressure. Therefore, our method is guaranteed to match with the experimental data near 298 K where most of the pressure deviation occurred. If the experimental pressure were to considerably deviate from the saturation pressure at elevated temperatures, then we would expect our estimation to be less accurate. In addition, caution should be made when employing this method with large solute molecules since it has been observed that pressure effects become more significant as the molar volume of the solute increases.[15]

From Figure 1 examining the proposed method, the relative errors in $\ln(K_{1,2}^{\infty}P)$ and solvation energy are generally similar for each solvent-solute pair. However, this is not always the case. In cases where the experimental pressure is greater than the saturation pressure of the solvent by even a small factor within 10 % of the critical temperature, the solvent's gas phase density at saturation pressure starts to deviate considerably from the density at experimental pressure. This causes the solvation energy to deviate even though the predicted K-factors match well with the experimental data. Four of the forty seven solvent-solute pairs have been found to exhibit such behavior and are highlighted in Figure 4. The experimental conditions that correspond to these outliers are listed in Table 2. However, note that the experimental solvation energies are estimates made using the solvent's densities calculated from the Helmholtz equations of state with dilute assumptions. These equations of state were not able to calculate the gas-phase densities for some of the experimental conditions, including three of the four pairs shown in Figure 4 (see the Supporting Information), either due to non-dilute conditions of experimental data or limitation of the equations of state themselves. This, in addition to the

pressure effect, may have contributed to the discrepancy between the accuracy of $\ln(K_{1,2}^{\infty}P)$ and solvation energy.

The comparison between the non-ideal and ideal gas density methods shown in Figure 2 reveals close agreement at low temperature and noticeable difference at high temperature near the critical point. The result meets our expectation as the ideal gas law is expected to fail at high pressure. Nonetheless, the method based on ideal gas density gives reasonably good solvation energy estimation for most of the temperature range and can be a useful alternative when the exact gas density is not known.

We also note that some of the solutes are expected to react or ionize in water. For example, carbon dioxide would be expected to equilibrate between the dissolved gas and carbonic acid. However, at equilibrium the amount existing in a state that is not the dissolved gas is expected to be insignificant[36] for a partial pressure of carbon dioxide greater than around 1000 Pa and as such was ignored in this treatment. Some other species, such as acetic and formic acid, while generally at concentrations high enough that the vast majority of the solute is not ionized, might have some data that are affected by ionization. Some hydrocarbons pyrolyze at significant rates below their critical points, and others might hydrolyze or hydrate. Care should be exercised when making predictions about these or other species that react upon solvation.

Although we compared the predicted values to the experimental data of binary systems only, we believe that our method will work for any gas mixtures dissolved in a single solvent in dilute limit. Additional errors are expected if any of the high concentration gases in the mixture are highly soluble in the solvent since this may violate the dilute solution in a pure solvent assumption. Nevertheless, the validating set includes experimental data in which the solute mole fractions in solvents deviate from dilute limit and reach as high as 0.4 in some cases (see the Supporting Information). No obvious correlation between the error and the solute mole fractions in solvents was found in our validation set, but the caution should be made when applying the proposed method to non dilute systems.

Note also that one could extract estimates of temperature dependent solvation entropy and enthalpy from the predicted free energy.

$$\Delta S^*_{solv}(T) = -\frac{d\Delta G^*_{solv}}{dT} \tag{24}$$

$$\Delta H^*_{solv}(T) = \Delta G^*_{solv} - T\frac{d\Delta G^*_{solv}}{dT} \tag{25}$$

We are not able to assess the reliability of these estimates due to the lack of validation data for ΔH^*_{solv} and ΔS^*_{solv} at high temperatures.

CONCLUSIONS

We have developed a method for predicting the temperature dependence of K-factors and solvation free energies for neutral solutes that balances speed and accuracy. This method outperforms existing low-cost extrapolation methods. We believe that this method will be especially appropriate in the automatic generation of liquid phase detailed chemistry models where the rapid estimation of properties is of paramount importance.

ACKNOWLEDGEMENTS

REFERENCES

1. Chamberlin AC, Cramer CJ, Truhlar DG. Predicting aqueous free energies of solvation as functions of temperature. *The Journal of Physical Chemistry B.* 2006;110(11):5665-5675.

2. Lin ST, Sandler SI. Infinite dilution activity coefficients from ab initio solvation calculations. *AIChE Journal.* 1999;45:2606-2618.

3. Guillot B, Guissani Y. A computer simulation study of the temperature dependence of the hydrophobic hydration. *J. Chem. Phys..* 1993;99:8075-8094.

4. Abraham MH. Scales of solute hydrogen-bonding: their construction and application to physicochemical and biochemical processes. *Chemical Society Reviews.* 1993;22:73-83.

5. Mintz C, Clark M, Acree WE, Abraham MH. Enthalpy of solvation correlations for gaseous solutes dissolved in water and in 1-octanol based on the Abraham model. *Journal of Chemical Information and Modeling.* 2007;47(1):115-121.

6. Klamt A. Conductor-like screening model for real solvents: a new approach to the quantitative calculation of solvation phenomena. *The Journal of Physical Chemistry.* 1995;99(7):2224-2235.

7. Maurer G, Prausnitz J. On the derivation and extension of the UNIQUAC equation. *Fluid Phase Equilibria.* 1978;2(2):91 - 99.

8. Skjold-Jorgensen S, Kolbe B, Gmehling J, Rasmussen P. Vapor-liquid equilibria by UNIFAC group contribution. Revision and extension. *Industrial & Engineering Chemistry Process Design and Development.* 1979;18(4):714-722.

9. Gmehling J, Li J, Schiller M. A modified UNIFAC model. 2. Present parameter matrix and results for different thermodynamic properties. *Industrial & Engineering Chemistry Research.* 1993;32(1):178-193.

10. Constantinescu D, Gmehling J. Further development of modified UNIFAC (Dortmund): revision and extension 6. *Journal of Chemical & Engineering Data.* 2016;61(8):2738–2748.

11. Plyasunov AV, Shock EL. Prediction of the vapor–liquid distribution constants for volatile nonelectrolytes in water up to its critical temperature. *Geochimica et Cosmochimica Acta*. 2003;67:4981-5009.

12. Plyasunov AV. Correlation and prediction of thermodynamic properties of nonelectrolytes at infinite dilution in water over very wide temperature and pressure ranges (2000K and 10GPa). *Geochimica et Cosmochimica Acta*. 2015;168:236-260.

13. Marenich AV, Cramer CJ, Truhlar DG. Universal solvation model based on solute electron density and on a continuum model of the solvent defined by the bulk dielectric constant and atomic surface tensions. *The Journal of Physical Chemistry B*. 2009;113:6378-6396.

14. Klamt A, Eckert F. COSMO-RS: a novel and efficient method for the a priori prediction of thermophysical data of liquids. *Fluid Phase Equilibria*. 2000;172:43-72.

15. Majer V, Sedlbauer J, Bergin G. Henry's law constant and related coefficients for aqueous hydrocarbons, CO_2 and H_2S over a wide range of temperature and pressure. *Fluid Phase Equilibria*. 2008;272:65-74.

16. Japas ML, Levelt Sengers JMH. Gas solubility and Henry's law near the solvent's critical point. *AIChE Journal*. 1989;35(5):705-713.

17. Harvey AH, Levelt Sengers JMH. Correlation of aqueous Henry's constants from $0°C$ to the critical point. *AIChE Journal*. 1990;36:539-546.

18. Harvey AH. Semiempirical correlation for Henry's constants over large temperature ranges. *AIChE Journal*. 1996;42(5):1491-1494.

19. Plyasunov AV, Shock EL. Prediction of the Krichevskii parameter for volatile nonelectrolytes in water. *Fluid Phase Equilibria*. 2004;222-223:19-24.

20. Abraham MH, Ibrahim A, Zissimos AM. Determination of sets of solute descriptors from chromatographic measurements. *Journal of Chromatography A*. 2004;1037:29-47.

21. Abraham MH, Poole CF, Poole SK. Classification of stationary phases and other materials by gas chromatography. *Journal of Chromatography A*. 1999;842:79-114.

22. Callihan BK, Ballantine DS. Calculation of Abraham solute descriptors from McReynolds gas chromatographic retention data. *Journal of Chromatography A*. 2000;893:339-346.

23. Platts JA, Butina D, Abraham MH, Hersey A. Estimation of molecular linear free energy relation descriptors using a group contribution approach. *J. Chem. Inf. Comput Sci.*. 1999;39(5):835-845.

24. Ulrich N, Endo S, Brown T, et al. UFZ-LSER Database v 3.2 [Internet]. `http://www.ufz.de/lserd`. 2017. Accessed February 19, 2020.

25. Ben-Naim A. *Solvation thermodynamics*. Plenum Press 1987.

26. Jalan A, Ashcraft RW, West RH, Green WH. Predicting solvation energies for kinetic modeling. *Annu. Rep. Prog. Chem., Sect. C: Phys. Chem.*. 2010;106:211-258.

27. Smith FL, Harvey AH. Avoid common pitfalls when using Henry's law. *Chemical Engineering Practice*. 2007;103:33-39.

28. Sander R. Compilation of Henry's law constants (version 4.0) for water as solvent. *Atmospheric Chemistry and Physics*. 2015;15(8):4399–4981.

29. Harvey AH, Crovetto R, Levelt Sengers JMH. Limiting vs. apparent critical behavior of Henry's constants and K factors. *AIChE Journal*. 1990;36(12):1901-1904.

30. Gao CW, Allen JW, Green WH, West RH. Reaction mechanism generator: automatic construction of chemical kinetic mechanisms. *Computer Physics Communications*. 2016;203:212-225.

31. Abraham MH. Personal Communication. 2019.

32. Bell IH, Wronski J, Quoilin S, Lemort V. Pure and pseudo-pure fluid thermophysical property evaluation and the open-source thermophysical property library CoolProp. *Industrial & Engineering Chemistry Research*. 2014;53(6):2498-2508.

33. COSMOtherm, <release 1901> . COSMOlogic GmbH & Co KG. `http://www.cosmologic.de`.

34. Dortmund Data Bank Software and Separation Technology GmbH, <Version 2014.03> . Dortmund Data Bank integrated in SpringerMaterials 2014. `https://materials.springer.com`. Accessed February 19, 2020.

35. Marenich AV, Kelly CP, Thompson JD, et al. Minnesota Solvation Database - version 2012. `https://comp.chem.umn.edu/mnsol/`. 2012. Accessed February 19, 2020.

36. Alan LS, Robert HB. CO2 system hydration and dehydration kinetics and the equilibrium CO2/H2CO3 ratio in aqueous NaCl solution. *Marine Chemistry*. 2002;78(2):65 - 73.

37. Shimoyama Y, Iwai Y, Yamada K, Yamakita M, Arai Y. Measurement and correlation of vapor-liquid equilibria for water + 2-propanol, water + 2-butanol, and water + 2-pentanol systems at high temperatures and pressures. *J. Chem. Eng. Data.* 2006;51:51–55.

38. Barr-David F, Dodge BF. Vapor-liquid equilibrium at high pressures the systems ethanol - water and 2-propanol - water. *J. Chem. Eng. Data.* 1959;4:107–121.

39. Rajendran M, Renganarayanan S, Srinivasan D. Salt effect in phase equilibria: effect of dissolved inorganic salts on the liquid-liquid equilibria of benzene-2-propanol-water system and the vapor-liquid equilibria of its constituent binaries. *Fluid Phase Equilib..* 1989;50:133–164.

40. Arce A, Arce A, Martinez-Ageitos J, Rodil E, Soto A. (Vapour + liquid) equilibrium of (DIPE+IPA+water) at 101.32 kPa. *J. Chem. Thermodyn..* 2003;35:871–884.

41. Ohe S, Yokoyama K, Nakamura S. Research on distillation using salt effect - isopropyl alcohol - water - calcium chloride system. *Kogyo Kagaku Zasshi.* 1969:313–316.

42. Choffe B, Asselineau L. Etude des equilibres liquides-vapeur entre l'acetone l'isopropanol et l'eau sous la pression de 760 mm de mercure. Premiere partie: etude des equilibres binaires.. *Rev. Inst. Francais Petrol..* 1956;11:948–954.

43. Yorizane M, Yoshimura S, Yamamoto T. Measurement of the ternary vapor-liquid equilibrium (isopropyl alcohol-water-isopropyl ether system). *Kagaku Kogaku.* 1967:451–457.

44. Lin CL, Lee LS, Tseng HC. Phase equilibria for propan-1-ol+water+sodium chloride and + potassium chloride and propan-2-ol + water+lithium chloride and +lithium bromide. *J. Chem. Eng. Data.* 1993;38:306–309.

45. Dobroserdov LL. Liquid-vapor phase equilibria in the system isopropyl alcohol-water-calcium chloride. *J. Appl. Chem. USSR.* 1959;32:2657–2660.

46. Li Q, Xing F, Lei Z, Wang B, Chang Q. Isobaric vapor-liquid equilibrium for isopropanol + water + 1-ethyl-3-methylimidazolium tetrafluoroborate. *J. Chem. Eng. Data.* 2008;53:275–279.

47. Wu W, Zhang Y, Wang Y, Shi J. Vapor-liquid equilibrium data for system 2-PrOH-H2O-KAc. *Shiyou-huagong.* 1997;26:610–613.

48. Gironi F, Lamberti L. VLE data for the water-2-propanol system in the presence of dissolved salts. *Fluid Phase Equilib..* 1995;105:273–286.

49. Kohoutova J, Suska J, Novak JP, Pick J. Liquid-vapor equilibrium XLV. System methanol-2-propanol water. *Collect.Czech. Chem. Commun..* 1970;35:3210–3222.

50. Ratkovics F, Sayed AR. Calculation of vapour-liquid equilibria and the heat of mixing in mixtures containing an associative component. II. The heat of mixing of the system isopropanol-water. *Magy. Kem. Foly..* 1970;76:195–197.

51. Sevgili LM, Senol A. Isobaric (vapour + liquid) equilibrium for (2-propanol + water + ammonium thiocyanate): fitting the data by an empirical equation. *J. Chem. Thermodyn..* 2006;38:1539–1545.

52. Brunjes AS, Bogart M. Vapor-liquid equilibria for commercially important systems of organic solvents: the binary systems ethanol-n-butanol, acetone-water and isopropanol-water. *Ind. Eng. Chem..* 1943;35:255–260.

53. Verhoeye LA. System cyclohexane-2-propanol-water. *J. Chem. Eng. Data.* 1968;13:462–467.

54. Gu F, Hou Y. Salt effects on the isobaric vapor-liquid equilibrium for four binary systems. *J. Chem. Eng. Data.* 2000;45:467–470.

55. Wu HS, Hagewiesche D, Sandler SI. Vapor-liquid equilibria of 2-propanol + water + n-dimethyl formamide. *Fluid Phase Equilib..* 1988;43:77–89.

56. Ramalho RS, Drolet JF. Vapor-liquid equilibria data for the ternary system acetone-2-propanol-water and corresponding binaries from total pressure measurements. *J. Chem. Eng. Data.* 1971;16:12–15.

57. Westerholt A, Liebert V, Gmehling J. Influence of ionic liquids on the separation factor of three standard separation problems. *Fluid Phase Equilib..* 2009;280:56–60.

58. Tunik EK, Zharov VT. Phasen- und chemische gleichgewichte im system ameisensaure-wasser-isopropylformiat-isopropanol. *Viniti.* 1980:1–16.

59. Marzal P, Monton JB, Rodrigo MA. Isobaric vapor-liquid equilibria of the water + 2-propanol system at 30, 60, and 100 kPa. *J. Chem. Eng. Data.* 1996;41:608–611.

60. Wilson A, Simons EL. Vapour-liquid equilibria. 2-propanol-water system. *Ind. Eng. Chem..* 1952;44:2214–2219.

61. Sada E, Morisue T. Isothermal vapor-liquid equilibrium data of isopropanol-water system. *J. Chem. Eng. Japan.* 1975;8:191–195.

62. Udovenko VV, Mazanko TF. Liquid-vapor equilibrium in the propan-2-ol-water and propan-2-ol-benzene systems. *Zh. Fiz. Khim..* 1967;41:1615–1618.

63. Sazonov VP. Isothermal equilibria of liquid-liquid vapor in the system nitromethane-isopropyl alcohol-water diphenyl-methane/toluene, m-cresol/1,2,3,4-tetrahydronaphthalene, and quinoline/benzene. *Zh. Prikl. Khim..* 1986;59:1451–1456.

64. Al-Ghamdi AM, Kabadi VN. High temperature VLE for benzene-ethylbenzene system. *J. Chem. Eng. Data.* 2001;46:1330–1332.

65. Kutsarov RK, Ralev ND, Sharlopov VK. Liquid-vapor phase equilibrium of binary C6-C8 aromatic hydrocarbon systems. *Zh. Prikl. Khim..* 1993;66:567–573.

66. Kesselman WD, Hollenbach GE, Myers AL, Humphrey AE. Vapor-liquid equilibrium data for benzene-alkylbenzene systems. *J. Chem. Eng. Data.* 1968;13:34–36.

67. Mann RS, Shemilt LW. Vapor-liquid equilibria at atmospheric pressure I. 1-butanol-toluene system. *J. Chem. Eng. Data.* 1963;8:189–190.

68. Chen G, Yan X, Han S, Ma Z, Wang Q. Phase equilibria under superatmospheric pressures for binary systems of cyclohexane, 1-butanol and toluene. *Huagong-Xuebao / CIESC J..* 1994;45:94–101.

69. Seetharamaswamy V, Subrahmanyam V, Chiranjivi C, Dakshinamurty P. Vapor-liquid equilibria for the systems: methylcyclohexane-n-butanol and toluene-n-butanol. *J. Appl. Chem..* 1969;19:258–262.

70. Darwish NA, Al-Khateib AA. Isobaric vapor-liquid equilibria of the system toluene + n-butanol at 94.0, 70.5, and 56.4 kPa. *Fluid Phase Equilib..* 1997;132:215–223.

71. Gropsianu Z, Kyri J, Gropsianu R. Echilibre lichid-vapori la presuni subatmosferice pentru sistemele: benzen-dioxan, dioxan-toluen, alcool etilic-dioxan si toluen-alcool n-butilic. *Stud. Cerc. ARPR. Baza Timisoara Ser. Sti. Chim..* 1957;4:73–85.

72. Lnenickova J, Wichterle I. Vapor-liquid equilibrium in toluene-aliphatic C4 alcohol systems. *Collect. Czech. Chem. Commun.* 1907;42.

73. Seo J, Lee J, Kim H. Isothermal vapor-liquid equilibria for ethanol and n-pentane system at the near critical region. *Fluid Phase Equilib..* 2000;172:211–219.

74. Campbell SW, Wilsak RA, Thodos G. (Vapor+ liquid) equilibrium behavior of (n-pentane + ethanol) at 372.7, 397.7, and 422.6 K. *J. Chem. Thermodyn..* 1987;19:449–460.

75. Ishii N. Studies on volatility of fuels containing ethyl alcohol V-VI. *J. Soc. Chem. Ind. Jap..* 1935;38:659.

76. Oh BC, Lee S, Seo J, Kim H. Isothermal vapor-liquid equilibria for the 2-propanol + n-heptane system near the critical region. *J. Chem. Eng. Data.* 2004;49:221–223.

77. Wisniak J, Apelblat A, Tamir A. Vapor-liquid equilibrium in the system 2-propanol-heptane. *J. Chem. Eng. Data.* 1980;25:113–115.

78. Sabarathinam PL, Andiappan AN. Isobaric vapor-liquid equilibria for binary systems: n-propanal, isopropanol, isobutanol and tert-butanol with n-heptane. *Indian J. Technol..* 1985;23:101–103.

79. Vijayaraghavan SV, Deshpande PK, Kuloor NR. Vapor equilibrium at atmospheric pressure. *Chem. Age India.* 1964;15:1016–1018.

80. Ciprian M, Vlaic GP. Determination and correlation of isobaric vapor liquid equilibrium data. *Advances in Separation Science.* 1978:210–216.

81. Cummings LWT, Stones FW, Volante MA. High pressure rectification II. n-pentane-n-heptane system. *Ind. Eng. Chem. Ind.* 1933;25:728–732.

82. Burova GV, Kogan VB, Nemtsov MS. Liquid-vapor equilibria in ternary and quaternary systems consisting of C5 hydrocarbons and separating agents. *J. Appl. Chem. USSR.* 1965;38:111–117.

83. Cummings LWT. *High pressure rectification.* [dissertation] 1933.

84. Seo J, Lee J, Kim H. Measurement and correlation of vapor-liquid equilibria for the 2-propanol + n-hexane system near the critical region. *J. Chem. Eng. Data.* 2003;48:856–859.

85. Kozhenkov AV, Sobolev DM, Malenko Y. Liquid-vapor equilibrium in the four-component acetone-hexane-isopropanol-toluene system. *Zh. Prikl. Khim..* 1989;62:1319–1322.

86. Govindaswamy S, Andiappan A, Lakshmanan S. Isobaric vapour-liquid equilibrium data for the ternary and sub-binary systems containing n-hexane(1) -benzene(2) - isopropanol(3). *J. Chem. Eng. Japan.* 1976;9:345–349.

87. Wisniak J, Akunis A. Isobaric vapor-liquid equilibria in the binary system hexane + 2-propanol. *J. Chem. Eng. Data.* 1995;40:920–923.

88. Berro C, Neau E, Rogalski M. Vapor-liquid equilibrium of the systems 1-propanol-2, 2, 4-trimethylpentane and 2-propanol-n-hexane. *Fluid Phase Equilib..* 1981;7:41–54.

89. Maciel MRW, Francesconi AZ. Excess Gibbs free energies of (n-hexane + propan-1-ol) at 338.15 and 348.15 K and of (n-hexane + propan-2-ol) at 323. 15 K. *J. Chem. Thermodyn.*. 1988;20:539–544.

90. Barraza R, Edwards J. Thermodynamics of the isopropanol-n-hexane and isopropanol-n-heptane systems part III. Gas/liquid equilibrium. *Monatsh. Chemie*. 1981;112:925–933.

91. Bekarek V. Liquid-vapour equilibrium. XL. Liquid-vapour equilibrium in the systems SO2-CH3COOH3-CH3OH and SO2-CH3COH3-CH3OH. *Collect. Czech. Chem. Commun.*. 1968;33:2608-2619.

92. Pierotti GJ, Deal CH, Derr EL. Activity coefficients and molecular structure. *Ind. Eng. Chem.*. 1959;51:95-102.

93. Tamir A, Apelblat A, Wagner M. An evaluation of thermodynamic analyses of the vapor-liquid equilibria in the ternary system acetone-chloroform-methanol and its binaries. *Fluid Phase Equilib.*. 1981;6:113-139.

94. Griswold J, Wong SY. Phase equilibria of the acetone-methanol-water system from 100°C into the critical region. *Chem. Eng. Prog. Symp. Ser.*. 1952;48:18–34.

95. Wilsak RA, Campbell SW, Thodos G. Vapor-liquid equilibrium measurements for the methanol-acetone system at 372 K. *Fluid. Phase. Equilib.*. 1986;28:13-37.

96. Kato M, Sato T, Konishi H, Hirata M. New method for measuring ternary vapor-liquid equilibria. *J. Chem. Eng. Japan*. 1971;4:311–318.

97. Dernini S, Santis R, Marelli L. Salt effects in isobaric vapor-liquid equilibria of acetone-methanol system. *J. Chem. Eng. Data*. 1976;21:170–173.

98. Orchilles AV, Miguel PJ, Vercher E, Martinez-Andreu A. Ionic liquids as entrainers in extractive distillation: isobaric vapor-liquid equilibria for acetone + methanol + 1-ethyl-3-methylimidazolium trifluoromethanesulfonate. *J. Chem. Eng. Data*. 2007;52:141-147.

99. Hiaki T, Kurihara K, Kojima K. Vapor-liquid equilibria for acetone + chloroform + methanol and constituent binary systems at 101. *J. Chem. Eng. Data*. 1994;39:714–719.

100. Amer HH, Paxton RR, Winkle M. Methanol-ethanol-acetone vapor-liquid equilibria. *Ind. Eng. Chem.*. 1956;48:142–146.

101. Tu CH, Wu YS, Liu TL. Vapor-liquid equilibria of the binary systems formed by methanol, acetone and methy vinyl ketone at 100°C. *Fluid Phase Equilib.*. 1997;2(129):129–137.

102. Uchida S, Ogawa S, Yamaguchi M. Studies in distillation. *Jap. Sci. Rev. Eng. Sci.*. 1950;1:41-49.

103. Harper BG, Moore JC. Vapor-liquid equilibrium: new still and method for determining vapor-liquid equilibrium. *Ind. Eng. Chem.*. 1957;49:411–414.

104. Avciata U, Teker M, Demiryuerek B. Salt effects in isobaric vapor-liquid equilibria of acetone - methanol system. *Modelling Measurement & Control C 44*. 1994:53–63.

105. Ochi K, Kojima K. Vapor-liquid equilibria for the system acetone + methanol + water. *Kagaku Kogaku*. 1971;35:583-586.

106. Al-Asheh S, Banat F. Isobaric vapor-liquid equilibrium of acetone + methanol system in the presence of calcium bromide. *J. Chem. Eng. Data*. 2005;50:1789-1793.

107. Yan W, Topphoff M, Zhu M, Gmehling J. Measurement and correlation of isobaric vapor-liquid equilibrium data for the system acetone + methanol + zinc chloride. *J. Chem. Eng. Data*. 1999;44:314-318.

108. Vercher E, Orchilles AV, Miguel PJ, Gonzalez-Alfaro V, Martinez-Andreu A. Isobaric vapor-liquid equilibria for acetone + methanol + lithium nitrate at 100 kPa. *Fluid Phase Equilib.*. 2006;250:131-137.

109. Freshwater DC, Pike KA. Vapor-liquid equilibrium data for systems of acetone-methanol isopropanol. *J. Chem. Eng. Data*. 1967;12:179-183.

110. Marinichev AN, Susarev MP. A study of liquid-vapor equilibrium in the acetone-methonal and acetone-cyclohexane systems at temperatures of 35, 45 and 55°C and a pressure of 760 mm Hg. *J. Appl. Chem. USSR*. 1965;38:371-375.

111. Campbell AN, Anand SC. Phase equilibria in the systems acetone - methanol, acetone - cyclohexane, methanol - cyclohexane, and acetone - methanol - cyclohexane. *Can. J. Chem.*. 1972;50:479–489.

112. Fordyce CR, Simonsen DR. Cellulose ester solutions evaporation in binary solvent mixtures. *Ind. Eng. Chem.*. 1949;41:104-111.
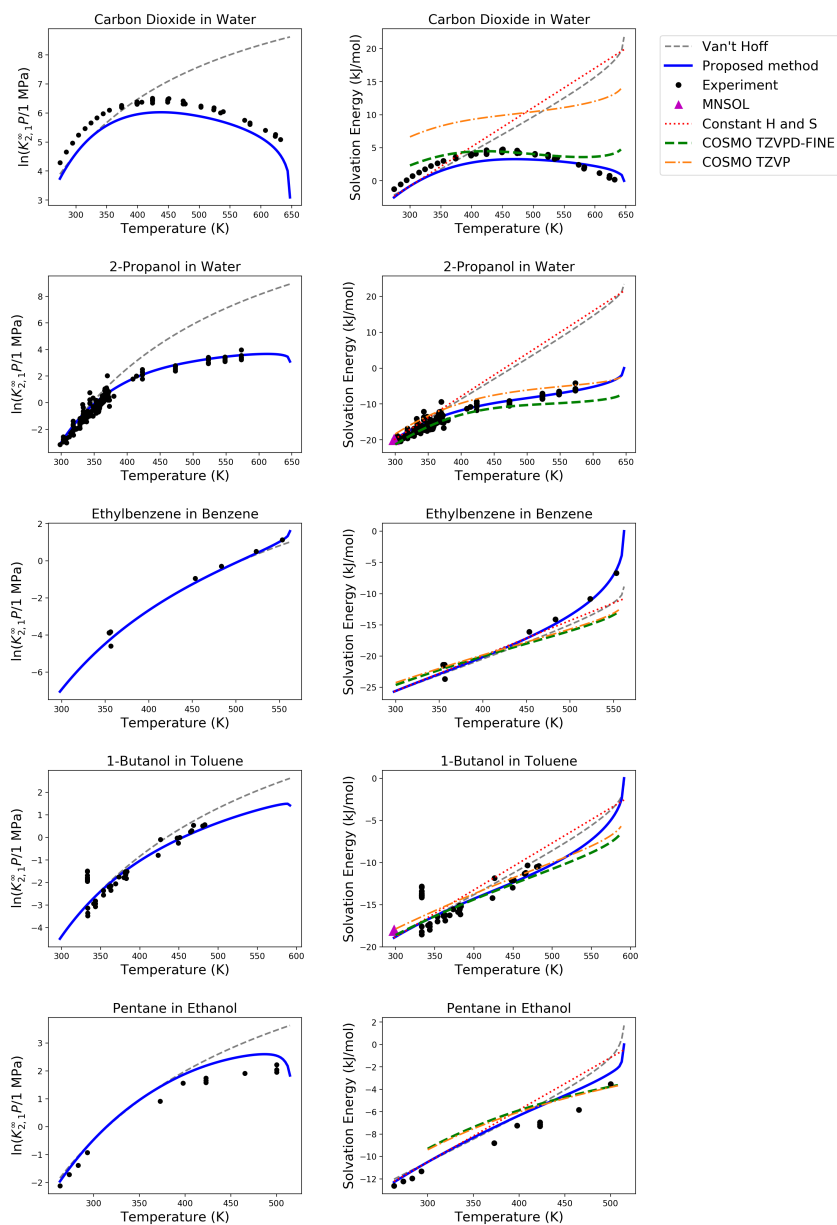
LIST OF FIGURES

FIGURE 1 A comparison of prediction methods on five solute-solvent pairs. The plots on the left and right columns show the temperature dependent $\ln(K_{1,2}^{\infty}P)$ and solvation free energy (ΔG_{solv}^{*}) respectively. All plots use the same legend. The proposed method uses the non-ideal gas density of the solvent for the conversion of K-factor to solvation energy. Experimental data: Carbon dioxide in water,[18] 2-Propanol in water[37 38 39 40 41 42 43 44 45 46 47 48 49 50 51 52 53 54 55 56 57 58 59 60 61 34 62],[63] Ethylbenzene in benzene[64 65],[66] 1-Butanol in toluene[67 68 69 70 71],[72] Pentane in ethanol[73 74 75]
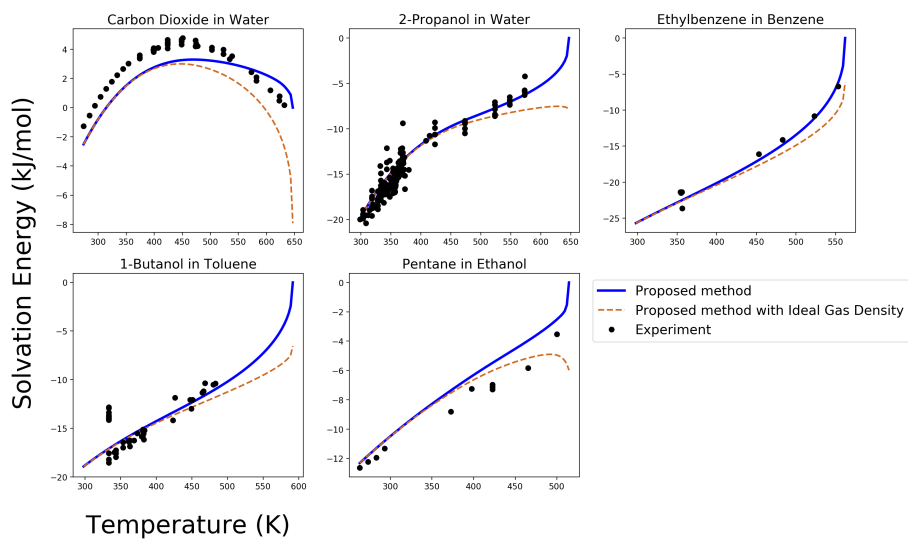
FIGURE 2   A comparison of solvation free energies (ΔG^*_{solv}) calculated using non-ideal and ideal gas densities on five solute-solvent pairs. The proposed method refers to the one using non-ideal gas density. Experimental data: Carbon dioxide in water,[18] 2-Propanol in water[37,38,39,40,41,42,43,44,45,46,47,48,49,50,51,52,53,54,55,56,57,58,59,60,61,34,62,63] Ethylbenzene in benzene[64,65,66] 1-Butanol in toluene[67,68,69,70,71,72] Pentane in ethanol[73,74,75]
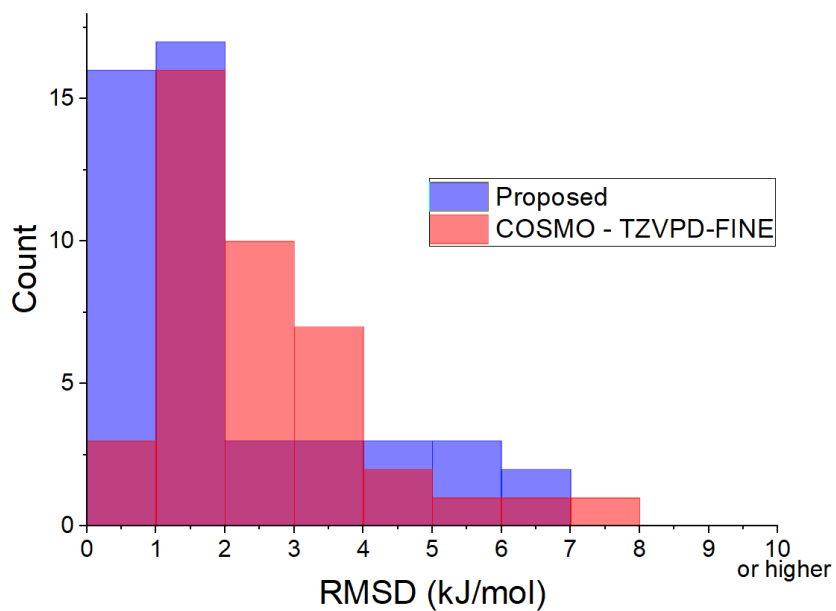
FIGURE 3   A histogram of the root mean squared deviation of solvation free energies (ΔG^{*}_{solv}) in kJ/mol between experiment and estimate for the proposed method using non-ideal gas density and the COSMO-RS BP/TZVPD-FINE model.
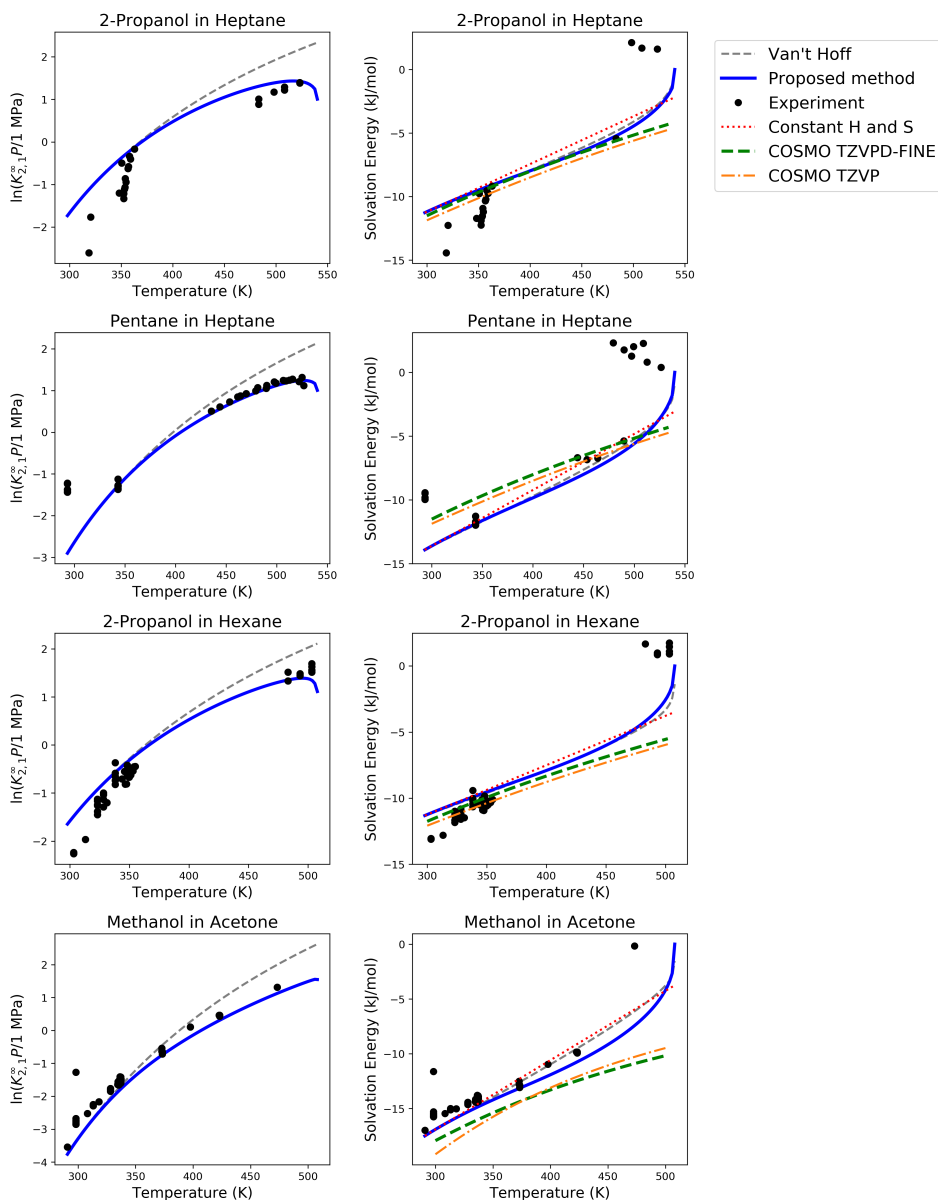
FIGURE 4 The cases where the predicted $\ln(K^{\infty}_{1,2}P)$ agrees with the experimental data and the predicted solvation energy ($\Delta G^{*}_{\text{solv}}$) does not. All plots use the same legend. Experimental data: 2-Propanol in heptane[76][77][78][79],[80] Pentane in heptane[81][82],[83] 2-Propanol in hexane[84][85][86][79][87][88][89],[90] Methanol in acetone[91][92][93][94][95][96][97][98][99][100][101][102][103][104][105][97][106][107][108][98][109][110][111][112]

Extrapolation Method								Ab Initio Method			
Proposed Method		Proposed Method: Ideal Gas Density		Constant Enthalpy and Entropy		Van't Hoff Equation		COSMO - TZVP		COSMO - TZVPD-FINE	
RMSD	MAD	RMSD	MAD	RMSD	MAD	RMSD	MAD	RMSD	MAD	RMSD	MAD
2.0	1.6	2.1	1.7	2.9	2.2	2.6	1.9	2.7	2.2	2.5	2.1

TABLE 1 A comparison of the root mean squared deviation and mean absolute deviation of the predicted solvation free energies (ΔG^*_{solv}) for each extrapolation and prediction method (kJ/mol). Each solute and solvent pair is weighted equally.

Solvent	Solute	T_{expt} (K)	% from T_c	P_{expt}/P_{sat}	Reference
Heptane	2-Propanol	498.15	7.8%	1.33	76
		508.15	5.9%	1.46	76
		523.15	3.1%	1.40	76
Heptane	Pentane	479.25	11.3%	1.40	83
		489.95	9.3%	1.56	81
		497.45	7.9%	1.74	83
		499.25	7.6%	1.35	81
		509.05	5.8%	1.16	81
		512.65	5.1%	1.66	81
		526.65	2.5%	1.35	81
Hexane	2-Propanol	483.15	4.9%	1.49	84
		493.15	2.9%	1.53	84
		493.15	2.9%	1.55	84
Acetone	Methanol	473.15	6.9%	1.44	94

TABLE 2 The experimental conditions for the solvation energy (ΔG^*_{solv}) outliers.